

AN HST/WFC3-UVIS VIEW OF THE STARBURST IN THE COOL CORE OF THE PHOENIX CLUSTER

MICHAEL McDONALD^{1*}, BRADFORD BENSON², SYLVAIN VEILLEUX^{3,4,5,6}, MARSHALL W. BAUTZ¹, AND
CHRISTIAN L. REICHARDT⁷

Draft version June 5, 2019

ABSTRACT

We present the results of *Hubble Space Telescope Wide Field Camera 3* observations of the core of the Phoenix Cluster (SPT-CLJ2344-4243) in five broadband filters spanning rest-frame 1000–5500Å. These observations reveal complex, filamentary blue emission, extending for >40 kpc from the brightest cluster galaxy. We observe an underlying, diffuse population of old stars, following an $r^{1/4}$ distribution, confirming that this system is somewhat relaxed. The spectral energy distribution in the inner part of the galaxy, as well as along the extended filaments, is a smooth continuum and is consistent with that of a star-forming galaxy, suggesting that the extended, filamentary emission is not due to a large-scale highly-ionized outflow from the central AGN, but rather a massive population of young stars. We estimate an extinction-corrected star formation rate of $798 \pm 42 M_{\odot} \text{ yr}^{-1}$, consistent with our earlier work based on low spatial resolution ultraviolet, optical, and infrared imaging. We argue that such a high star formation rate is not the result of a merger, as it would require >10 mergers with gas-rich galaxies and there is no evidence for such multiple merger events. Instead, we propose that the high X-ray cooling rate of $\sim 2850 M_{\odot} \text{ yr}^{-1}$ is the origin of the cold gas reservoir. The combination of such a high cooling rate and the relatively weak radio source in the cluster core suggests that feedback has been unable to halt runaway cooling in this system, leading to this tremendous burst of star formation.

1. INTRODUCTION

The cores of galaxy clusters represent one of the few places in the Universe where large-scale cooling and feedback processes can be readily observed. Unlike isolated massive galaxies, where some of the energy injected into the interstellar medium (ISM) from the active galactic nucleus (AGN) often escapes into the low-density intergalactic medium (IGM), the denser intracluster medium (ICM) in cluster cores retains an imprint of this feedback in the form of cavities (e.g., Birzan et al. 2004; Hlavacek-Larrondo et al. 2012) or ripples (e.g., Perseus A; Fabian et al. 2003). Similarly, the accretion of hot gas from the IGM onto massive galaxies is challenging to observe due to the very low densities, while such phenomena have been studied in depth for decades in galaxy clusters. These so-called “cooling flows” in galaxy clusters, which were once thought to be massive flows of cool gas on the order of 100–1000 $M_{\odot} \text{ yr}^{-1}$ (see review by Fabian 1994), are now understood to be considerably less massive, depositing on the order of 1–10 $M_{\odot} \text{ yr}^{-1}$ of cool gas onto the brightest cluster galaxy (BCG). This resid-

ual cooling has been detected in UV spectra (O VI lines; e.g., Oegerle et al. 2001; Bregman et al. 2006), warm ionized gas (e.g., Hu et al. 1985; Crawford et al. 1999; McDonald et al. 2010, 2011a), warm molecular gas (e.g., Jaffe et al. 2005; Donahue et al. 2011), cold molecular gas (e.g., Edge 2001; Edge et al. 2002; Salomé & Combes 2003; McDonald et al. 2012b), and via young stars detected in the far UV (e.g., McDonald et al. 2011b) and mid infrared (e.g., O’Dea et al. 2008; Rawle et al. 2012). The exact feedback mechanism that prevents the cooling catastrophe from happening, allowing only a few percent of the predicted cooling flow to reach low ($< 10^4\text{K}$) temperatures, is still not fully understood. The leading hypothesis of mechanical AGN-driven feedback is supported by the strong correlation between the total energy required to offset cooling and the amount of radio power required to inflate X-ray cavities (McNamara & Nulsen 2007; Fabian 2012; McNamara & Nulsen 2012).

Recently, McDonald et al. (2012a) reported the unique properties of a galaxy cluster at $z = 0.596$, SPT-CLJ2344-4243 (hereafter the Phoenix Cluster), which was initially discovered by the South Pole Telescope using the Sunyaev Zel’dovich effect (Williamson et al. 2011). This cluster is among the most massive ($M_{200, Y_X} \sim 2.5 \times 10^{15} M_{\odot}$) and X-ray luminous ($L_{2-10\text{keV}} = 8.2 \times 10^{45} \text{ erg s}^{-1}$) yet discovered. In the central ~ 100 kpc, there is a dense, highly-luminous cool core, with a classical cooling rate ($\frac{dM}{dt} = \frac{2L_{\text{cool}}}{5kT}$) higher than any known cluster, at $3820 M_{\odot} \text{ yr}^{-1}$. Surprisingly, while most nearby cool core clusters convert only a few percent of the classical cooling flow into stars, the central galaxy in the Phoenix cluster appears to be experiencing a $740 M_{\odot} \text{ yr}^{-1}$ starburst, corresponding to roughly 20% of the predicted cooling flow. However, the central galaxy also contains a powerful AGN which

¹ Kavli Institute for Astrophysics and Space Research, MIT, Cambridge, MA 02139, USA

² Kavli Institute for Cosmological Physics, University of Chicago, 5640 South Ellis Avenue, Chicago, IL 60637, USA

³ Department of Astronomy, University of Maryland, College Park, MD 20742, USA

⁴ Joint Space-Science Institute, University of Maryland, College Park, MD 20742, USA

⁵ Astroparticle Physics Laboratory, NASA Goddard Space Flight Center, Greenbelt, MD 20771, USA

⁶ Max-Planck-Institut für extraterrestrische Physik, Postfach 1312, D-85741 Garching, Germany

⁷ Department of Physics, University of California, Berkeley, CA 94720, USA

* Email: mcdonald@space.mit.edu

† Hubble Fellow

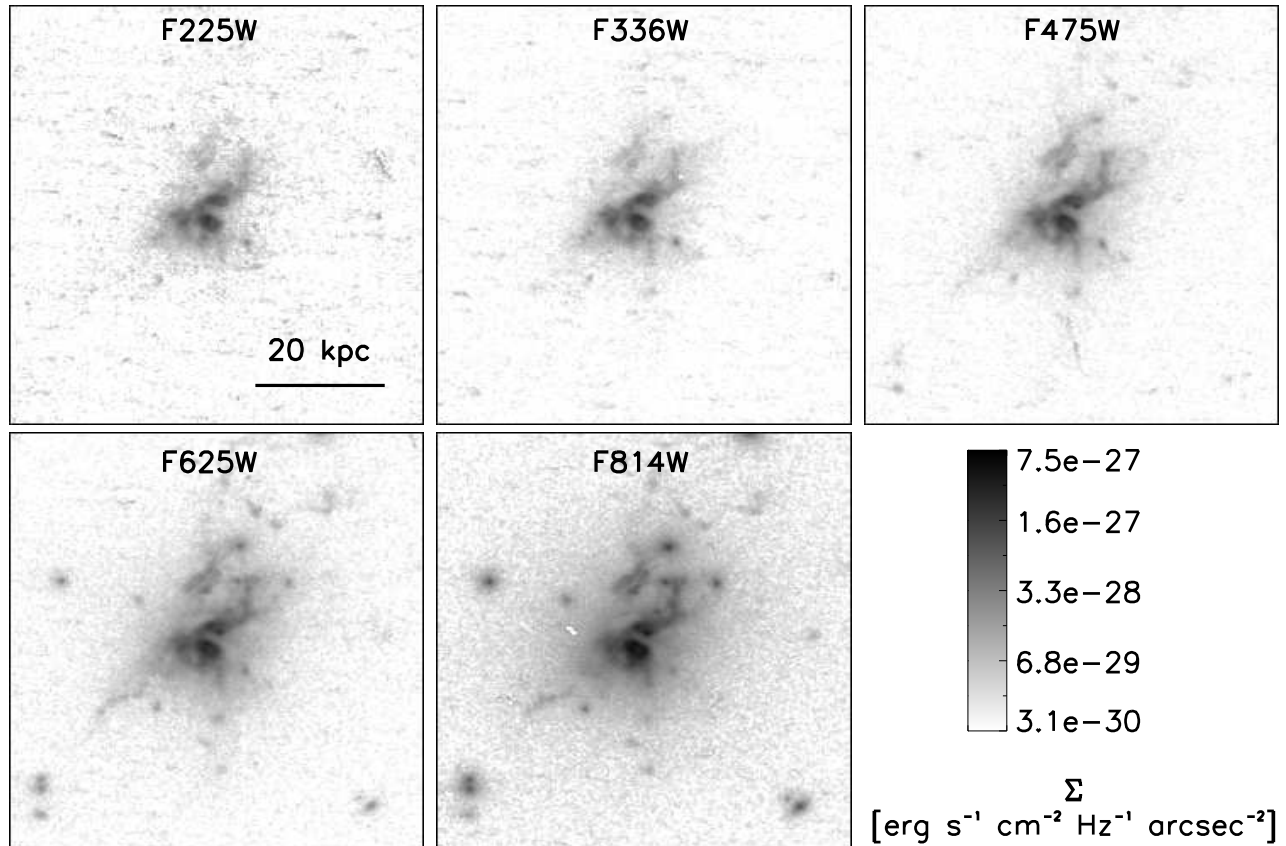


FIG. 1.— HST-WFC3 images of the core of the Phoenix cluster, in 5 different optical bands (rest-frame 1000–5500Å). These images highlight the complex morphology of the BCG. The presence of extended emission in all bands argues in favor of continuum, rather than line, emission. The full extent of these filaments, ~ 40 kpc, is reminiscent of those observed in nearby cool core clusters such as Perseus and Abell 1795.

makes it difficult to separate contributions to the ultraviolet, optical, and infrared emission from star-forming regions versus the AGN in low-resolution imaging. Further, the available ground-based data optical and space-based ultraviolet (UV) and infrared (IR) data presented in McDonald et al. (2012a) were unable to distinguish between in situ star formation (i.e., cooling flows), or the late stages of a merger.

In this Letter, we present new *Hubble Space Telescope* observations which improve significantly in depth and spatial resolution on the data presented in McDonald et al. (2012a). In §2 we describe these data and our analysis, after which we present our new, detailed view of the Phoenix cluster in §3. In §4 we discuss the possible interpretations of these data, including whether or not we can separate the cooling flow scenario from a pure AGN or merger scenario. We conclude with a summary of these results in §5. Throughout this letter we assume $H_0 = 70.2 \text{ km s}^{-1} \text{ Mpc}^{-1}$, $\Omega_M = 0.278$, and $\Omega_\Lambda = 0.728$.

2. HST DATA

To study in detail the purported starburst in the core of the Phoenix cluster, we obtained broadband imaging with the *Hubble Space Telescope Wide Field Camera 3* (HST WFC3) in five optical filters - F225W, F336W, F475W, F625W, F814W - which span rest-frame wavelengths from $\sim 1000\text{\AA}$ to $\sim 5500\text{\AA}$. These observations were carried out over 2 orbits of Director’s Discretionary

Time, with an average exposure time of ~ 1800 s per filter (PID #13102, PI McDonald).

In each filter, a series of two dithered exposures were obtained. The LA Cosmic¹⁰ (van Dokkum 2001) software was run on individual exposures, generating accurate cosmic ray and bad pixel masks for each image. Pairs of exposures were then combined using the PYRAF ASTRODRIZZLE routine¹¹, with the aforementioned masks preceding the standard cosmic ray detection in the MULTIDRIZZLE task. The final, cleaned images are presented in Figure 1.

All optical and UV fluxes were corrected for Galactic extinction following Cardelli et al. (1989) using a Galactic reddening estimate of $E(B - V) = 0.017$ towards the cluster center, from Schlegel et al. (1998).

3. RESULTS

In Figure 1 we show the newly-acquired far-UV through optical HST images of the core of the Phoenix cluster, which provide a detailed picture of this exotic system. These images show significant, extended filamentary emission at all wavelengths from ~ 1000 – 5500\AA , overlaid on a relatively smooth population of older, red stars. The most extended pair of filaments to the north of the BCG are $\sim 6''$ (40 kpc) in length, similar to the most extended filaments seen in Abell 1795

¹⁰ <http://www.astro.yale.edu/dokkum/lacosmic/>

¹¹ http://www.stsci.edu/hst/HST_overview/drizzlepac

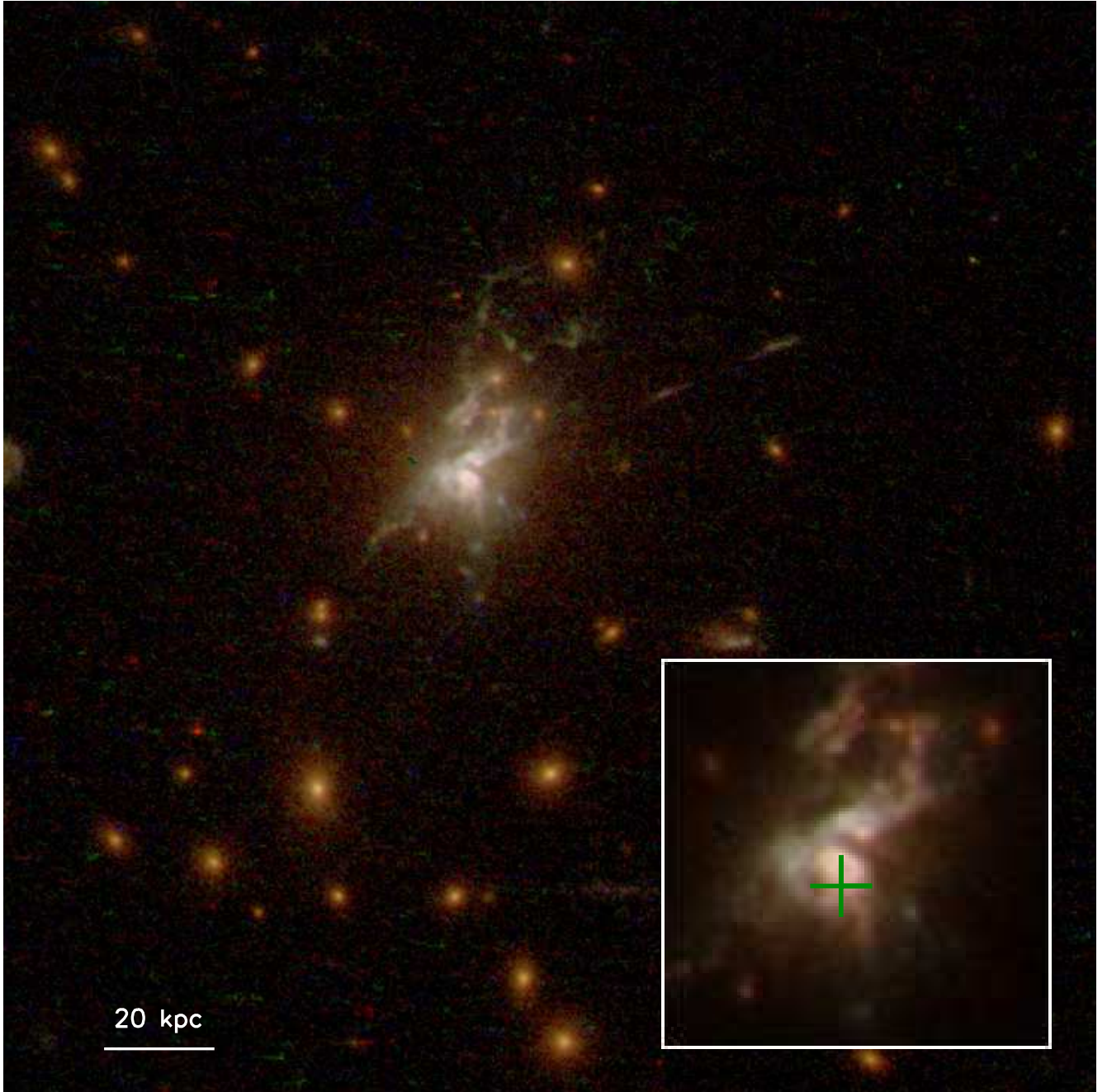


FIG. 2.— Color image, combining the F475W, F625, and F814W bands, showing the young, filamentary, star-forming regions overlaid on the diffuse, old stellar component of the BCG. In the inset we show the central ~ 20 kpc, with the position (and uncertainty) of the X-ray point source in green. There appear to be gaps in the emission to the northwest and southeast of the peak, possibly due to strong dust lanes.

(McDonald & Veilleux 2009), and the Perseus cluster (Conselice et al. 2001; Fabian et al. 2008). We measure a total rest-frame far-UV flux density of $f_{F225W} = 1.26 \times 10^{-27} \text{ erg s}^{-1} \text{ cm}^{-2} \text{ Hz}^{-1}$, consistent with the GALEX-derived flux presented in McDonald et al. (2012a).

The fact that such complex, filamentary morphology is present in all five filters suggests that the BCG is forming stars at a prodigious rate. In the wavelength range covered, there may be contributing emission from the Ly α (F225W), [O II] (F625W), and [O III] (F814W) lines. However, the F336W and F475W bands, which have sim-

ilar surface brightnesses to the other three bands, should be relatively free from emission lines, suggesting that ionized gas is not the dominant source of the observed flux in Figure 1.

In Figure 2 we show a three-color (F475W, F625W, F814W) image of the cluster core. This figure shows a clear difference in the stellar populations between the young (blue) filaments and the underlying, smoothly-distributed, old (red) stars. The peak of the emission in all bands is coincident (within the positional uncertainties) with the X-ray point source. To the northwest and southeast of the emission peak are dark lanes, most likely

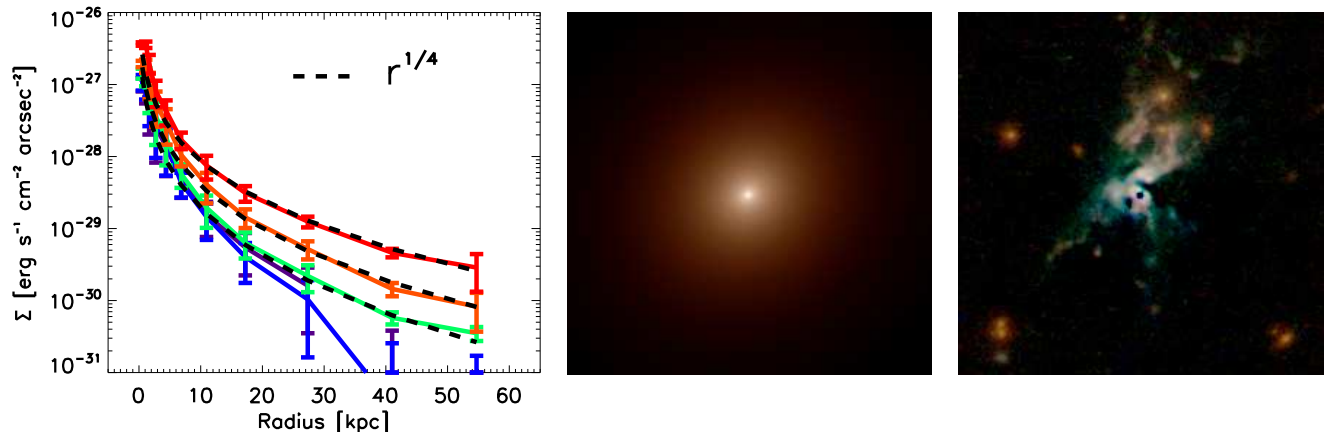


FIG. 3.— Left: Surface brightness profiles of the BCG in all five bands (purple: F225W, blue: F336W, green: F475W, orange: F625W, red: F814W). Each profile represents the average along four radial cuts with orientations chosen to avoid most of the extended, filamentary emission. The diffuse, red component of the BCG has a surface brightness distribution typical of an elliptical galaxy, well modeled by a $r^{1/4}$ fall-off in surface brightness (dashed line; de Vaucouleurs 1948). Middle: 2-dimensional surface brightness model from GALFIT (Peng et al. 2010), with ellipticity and PA of 0.88 and -52° , respectively. Right: Residual image generated by subtracting the $r^{1/4}$ model from each of the three reddest bands. Both color images use the same color scaling as Figure 2. This figure highlights the complex morphology of the star-forming filaments superimposed on the smooth, old stellar population in the BCG.

due to obscuration by dust. Overall, the color of the filamentary emission appears roughly constant with radius, and is reminiscent of a young, star-forming galaxy. We see no evidence for multiple bulges or tidal features, both of which would indicate that this system is the result of a recent merger of gas-rich galaxies.

In addition to the complex, filamentary emission, we observe two radial features to the northwest of the central galaxy, at a location >60 kpc from the X-ray peak. We interpret these as two radial arc candidates, background galaxies gravitationally lensed by the BCG of the Phoenix cluster. A more thorough analysis of the cluster potential is required to assess this interpretation, which is beyond the scope of this letter.

Figure 3 we shows the multi-band surface brightness profiles of the BCG (left panel), which have been computed along radial cuts at four different angles (90° , 120° , 180° , 210°), chosen to avoid the blue, filamentary emission. The profile follows a $r^{1/4}$ profile, which is typical of relaxed, early-type galaxies (de Vaucouleurs 1948). Projecting these 1-dimensional profiles back onto the sky, we can separate diffuse, giant elliptical emission (middle panel) from clumpy, star-forming emission (right panel). This confirms that the star-forming filaments do not resemble merging disk galaxies: there is a notable absence of smooth, arcing tidal features and multiple-bulges. We note that such $r^{1/4}$ surface brightness distributions are also common in the final stages (single-nucleus) of gas-rich mergers (ULIRGs; Veilleux et al. 2002, 2006). However, in contrast to local ULIRGs, this BCG is a factor of ~ 4 larger in size (Veilleux et al. 2002), a factor of ~ 60 higher in stellar mass (Veilleux et al. 2006), and resides in an environment ~ 50 – 100 times richer than normal (Zauderer et al. 2007). These factors argue that the Phoenix BCG is unlike a traditional local ULIRG by any definition other than the high total infrared luminosity.

In Figure 4 we provide the spectral energy distribution (SED) in several representative regions around the BCG. The diffuse emission at large and small radii indicate a significant positive age gradient in the diffuse population.

At large ($r \sim 40$ kpc) radii, the diffuse emission is consistent with a 2–5 Gyr old elliptical galaxy, while at smaller radii (~ 20 kpc) the diffuse stellar populations are much younger, similar in color to a star-forming late-type spiral galaxy. The extended, morphologically-complex filaments, after subtraction of the diffuse stellar component, show an excess of UV emission at all radii. The SED of the brightest filaments appear remarkably similar to the diffuse component in the central region, suggesting that these stars are being mixed on short timescales. In the faintest, most extended filaments, there is a substantial excess of emission in the F225W filter, at the location of the redshifted Ly α line, suggesting that these filaments may also contain warm ($> 10^4$ K), ionized gas. The overall flatness of the SED in the UV-bright regions is exactly what one would expect for a mix of young stars and warm, ionized gas, given the width of the broadband filters. At the peak of the optical emission, coincident with the X-ray source, the SED is well matched by a dusty type-2 QSO (Polletta et al. 2007), which is consistent with our X-ray observations of a highly-reddened hard X-ray point source. Finally, we find that the linear features to the northwest of the BCG (Figure 2) is inconsistent with synchrotron emission, suggesting that it is either an exceptionally linear filament or a gravitational arc.

The combination of Figures 1–4 paint a picture of an old, giant elliptical galaxy that is experiencing a resurgence of star formation. Below we re-evaluate the SFR in this system and describe various scenarios to explain this star-forming activity, building on the discussion of McDonald et al. (2012a).

4. DISCUSSION

The deep, high spatial resolution HST UV and optical imaging presented in §3 have revealed an exceptionally complex system. Below we utilize this improved spatial resolution to estimate a new, UV-derived SFR for the BCG in the Phoenix cluster, followed by a discussion of three possible origins for the extended, filamentary UV emission.

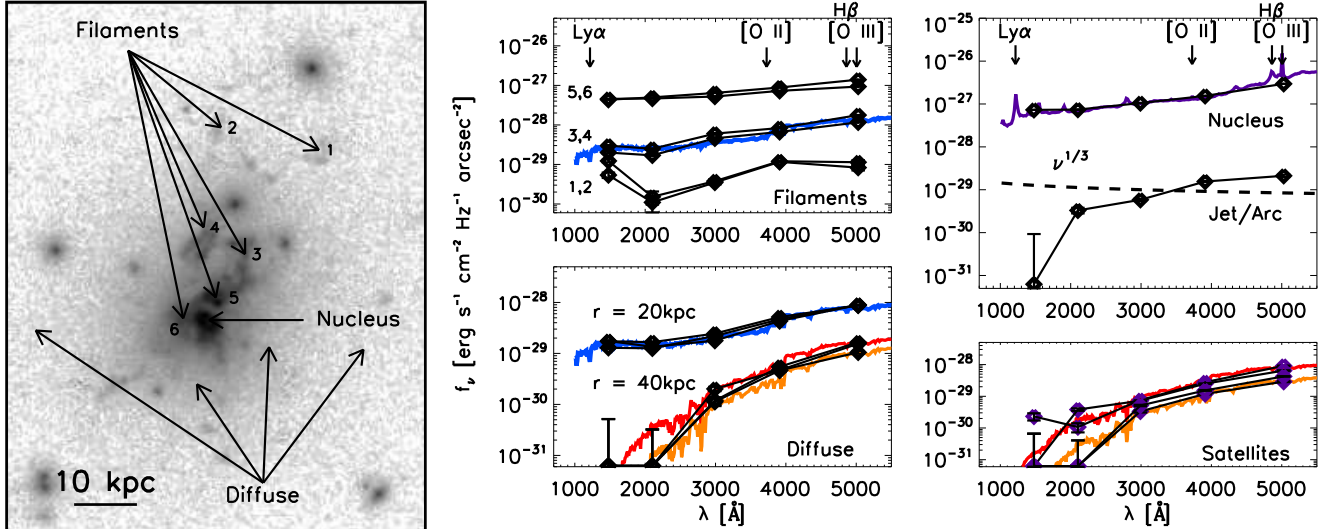


FIG. 4.— Left: F814W image of the Phoenix BCG, with positions of nucleus, filaments, and diffuse emission indicated. Right: SEDs for the different regions indicated on the left. For comparison, we also show the SEDs for four nearby early-type satellite galaxies. Orange and red spectra correspond to passive stellar populations of ages 2 and 5 Gyr, respectively, while blue and purple spectra correspond to a typical late-type spiral galaxy (Sdm) and dusty type-2 QSO, respectively (Polletta et al. 2007). All model spectra are normalized by eye. The faintest (labels 1 and 2) filaments show evidence for nebular emission, with peaks in the F225W and F625W bands, consistent with Ly α and [O II] emission. This figure confirms that, at large radii the stellar populations are typical for an early-type galaxy, while at small radii both the diffuse and filamentary emission result from significantly younger stellar populations. We also see that the UV-optical SED of the nucleus is consistent with a dusty AGN, while the linear feature to the northwest is inconsistent with synchrotron emission from a jet.

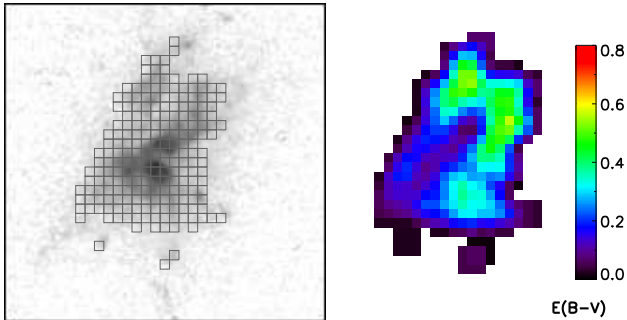


FIG. 5.— Left: Image in the F475W band, with $0.2'' \times 0.2''$ bins overlaid in regions with $> 5\sigma$ detections in both the F336W and F475W bands. Right: Smoothed reddening map, derived assuming a flat UV SED in the absence of reddening (Kennicutt 1998). This map allows us to perform *local* reddening corrections on the UV images, yielding a more tightly constrained estimate of the extinction-corrected UV luminosity.

4.1. A Revised Estimate of the SFR

The SFR reported in McDonald et al. (2012a), while utilizing an array of multi-wavelength data, necessarily required multiple assumptions to remove AGN contamination. With the addition of high-resolution HST UV imaging, we avoid such assumptions, leaving only the (typical) assumptions of dust extinctions and star formation laws.

To estimate the reddening, we assume that the reddening-free SED is flat at 1500–3000Å (Kennicutt 1998). Since the F225W filter is likely contaminated by Ly α emission, we use the mean f_{F336W}/f_{F475W} (rest frame f_{210}/f_{298}) flux ratio to derive a reddening correction, assuming $f_{F336W}/f_{F475W} = 1$ for $E(B-V) = 0$. In Figure 5 we show the spatial distribution of the reddening, $E(B-V)$, over regions with significant ($S/N > 5$) UV flux. We note that the mean reddening in this map agrees well with the reddening presented in McDonald et al.

(2012a) from Balmer line ratios ($E(B-V) = 0.34$). Using the *local* reddening correction and uncertainty we can accurately correct the UV luminosity, resulting in a more confident estimate of $L_{2000} = 5.7 \pm 0.3 \times 10^{30}$ erg s $^{-1}$ and a UV-derived SFR of 798 ± 42 M $_{\odot}$ yr $^{-1}$ (Kennicutt 1998).

We note that this estimate is consistent with the AGN-subtracted SFR quoted in McDonald et al. (2012a) of 739 ± 160 M $_{\odot}$ yr $^{-1}$ and with the empirical, extinction-implicit, method of Rosa-González et al. (2002), which yields $SFR_{UV} = 1040^{+1290}_{-580}$ M $_{\odot}$ yr $^{-1}$.

4.2. Possible Sources of Extended UV Emission

4.2.1. AGN-driven Outflow

Inspired by the high far-infrared luminosity, coupled with the hard X-ray and radio point source, a viable explanation for the data presented by McDonald et al. (2012a) is a dusty AGN driving a large-scale outflow (e.g., IRAS 09104+4109; O’Sullivan et al. 2012). While there certainly is a powerful AGN in the core of the Phoenix cluster, the new HST data suggest that the substantial UV luminosity can not be fully attributed to this AGN. Figure 1 shows that only a small fraction ($< 10\%$) of the total UV luminosity originates from a central point source, with the majority originating from extended, filamentary regions. Furthermore, the high relative fluxes in the F336W and F475W bands, which should be free from line emission, suggest that the majority of the UV/optical flux in these complex filaments is continuum emission. Finally, while the central galaxy does not appear to host a disk, it does appear elongated in the diffuse component ($b/a \sim 0.8$) towards the northwest ($PA \sim -40^{\circ}$), in the same direction as the extended filaments. There is a general lack of UV/blue emission along the minor axis of the central galaxy, contrary to what is typically observed in wide-angle AGN-driven outflows

(Veilleux et al. 2005). Thus, we argue that the filamentary UV emission does not result from an outflow.

4.3. Gas Rich Merger(s)

The far-IR luminosity ($L_{FIR} = 9.5 \pm 1.1 \times 10^{12} L_{\odot}$; McDonald et al. 2012a) of the BCG in the Phoenix cluster is significantly higher than the threshold ($>10^{12} L_{\odot}$) to be called an ultraluminous infrared galaxy (ULIRG; Sanders & Mirabel 1996), and pushing into “hyperluminous” territory (HyLIRG; $>10^{13} L_{\odot}$). The majority of ULIRGs appear to be late-stage mergers of gas-rich galaxies ($\sim 95\%$; Veilleux et al. 2002).

In a merger scenario, all of the cold gas would have to come from one or more infalling gas-rich galaxies, assuming that the giant elliptical galaxy was gas-poor to begin with. Following Hopkins et al. (2008), we assume that the peak star formation happens during the “coalescence/ULIRG” stage, and that this star formation is roughly constant over 100 Myr. Assuming $SFR = 800 M_{\odot} \text{ yr}^{-1}$, and 100% efficiency of star formation (being conservative), we estimate that the total mass of cold gas required would be $8 \times 10^{10} M_{\odot}$. From Boselli et al. (1997), gas-rich spiral galaxies in the cluster environment have typical cold gas masses of $M_{H_2} = 10^{8.9 \pm 0.4} M_{\odot}$, implying that we would need ~ 100 “typical” disk galaxies, or ~ 10 exceptionally gas-rich galaxies to fulfill our conservative requirements for fuel. In the latter case, the question of how such gas rich galaxies make into the dense cluster core without being stripped further compounds the problem.

These arguments, combined with the fact that this BCG is unlike “typical” ULIRGs in size, stellar mass, and environment (§3) suggest that the high SFR is not a result of gas-rich mergers.

4.4. Runaway Cooling of the Intracluster Medium

Our preferred explanation in McDonald et al. (2012a) was that the star formation in the cluster core is being fueled by gas cooling out of the ICM. This remains the most plausible avenue for such a large amount of cold gas to reach the core of the cluster, and is supported by the exceptionally bright X-ray cool core and relatively weak radio source. Such an imbalance between cooling and feedback could lead to runaway cooling, fueling bursts of star formation.

Following White et al. (1997), we estimate from the

X-ray data the mass deposition rate of the cooling flow, combining the X-ray cooling luminosity with the gravitational potential of the cluster in order to correct for gravitational work done as the gas falls towards the cluster center. We obtain an ICM cooling rate of $\dot{M} = 2850 M_{\odot} \text{ yr}^{-1}$ which is enough to fuel a $798 M_{\odot} \text{ yr}^{-1}$ starburst, assuming the feedback mechanism that prevents star formation in nearby clusters is operating less efficiently in Phoenix. In the future, high resolution X-ray spectroscopy of the cool core (e.g., Peterson & Fabian 2006) will provide firm estimates of the ICM cooling rate down to low temperatures, revealing whether or not this scenario is a plausible fuel source for this massive starburst.

5. SUMMARY AND CONCLUSIONS

We report new HST observations of the Phoenix cluster (SPT-CLJ2344-4243) with WFC3-UVIS in five filters covering rest-frame wavelengths 1000-5500Å. The high spatial resolution of HST is able to separate bright UV emission from the AGN and the surrounding diffuse, extended emission, definitively confirming the presence of a starburst in the BCG. The morphology of this central galaxy is complex, with narrow filaments extending for >40 kpc, reminiscent of the nearby Perseus and Abell 1795 clusters. We argue that the majority of the observed UV emission is due to young stars, on the basis of the complex morphology and flat SED over the wavelength range 1000–5500Å. We confirm the high SFR presented in McDonald et al. (2012a), measuring an extinction-corrected, AGN-removed UV-derived SFR of $798 \pm 42 M_{\odot} \text{ yr}^{-1}$. We find that merger driven scenarios would require an unreasonably large number of gas rich galaxies to supply the cold gas reservoir required to fuel the starburst, and conclude that the starburst is likely fueled by a runaway cooling flow.

ACKNOWLEDGEMENTS

We thank the HST Director for graciously providing the data for this program. M. M. acknowledges support provided by NASA through a Hubble Fellowship grant from STScI. S.V. acknowledges support from a Senior NPP Award held at NASA-GSFC and from the Humboldt Foundation to fund a long-term visit at MPE in 2012. BAB is supported by the National Science Foundation through grant ANT-0638937, with partial support provided by NSF grant PHY-1125897, the Kavli Foundation, and Chandra Award Number 13800883 issued by the Chandra X-ray Observatory Center.

REFERENCES

- Birzan, L., Rafferty, D. A., McNamara, B. R., Wise, M. W., & Nulsen, P. E. J. 2004, ApJ, 607, 800
- Boselli, A., Gavazzi, G., Lequeux, J., Buat, V., Casoli, F., Dickey, J., & Donas, J. 1997, A&A, 327, 522
- Bregman, J. N., Fabian, A. C., Miller, E. D., & Irwin, J. A. 2006, ApJ, 642, 746
- Cardelli, J. A., Clayton, G. C., & Mathis, J. S. 1989, ApJ, 345, 245
- Conselice, C. J., Gallagher, III, J. S., & Wyse, R. F. G. 2001, AJ, 122, 2281
- Crawford, C. S., Allen, S. W., Ebeling, H., Edge, A. C., & Fabian, A. C. 1999, MNRAS, 306, 857
- de Vaucouleurs, G. 1948, Annales d’Astrophysique, 11, 247
- Donahue, M., de Messières, G. E., O’Connell, R. W., Voit, G. M., Hoffer, A., McNamara, B. R., & Nulsen, P. E. J. 2011, ApJ, 732, 40
- Edge, A. C. 2001, MNRAS, 328, 762
- Edge, A. C., Wilman, R. J., Johnstone, R. M., Crawford, C. S., Fabian, A. C., & Allen, S. W. 2002, MNRAS, 337, 49
- Fabian, A. C. 1994, ARA&A, 32, 277
- . 2012, ArXiv e-prints
- Fabian, A. C., Johnstone, R. M., Sanders, J. S., Conselice, C. J., Crawford, C. S., Gallagher, III, J. S., & Zweibel, E. 2008, Nature, 454, 968
- Fabian, A. C., Sanders, J. S., Allen, S. W., Crawford, C. S., Iwasawa, K., Johnstone, R. M., Schmidt, R. W., & Taylor, G. B. 2003, MNRAS, 344, L43

- Farrah, D., Verma, A., Oliver, S., Rowan-Robinson, M., & McMahon, R. 2002, *MNRAS*, 329, 605
- Hlavacek-Larrondo, J., Fabian, A. C., Edge, A. C., Ebeling, H., Sanders, J. S., Hogan, M. T., & Taylor, G. B. 2012, *MNRAS*, 421, 1360
- Hopkins, P. F., Hernquist, L., Cox, T. J., & Kereš, D. 2008, *ApJS*, 175, 356
- Hu, E. M., Cowie, L. L., & Wang, Z. 1985, *ApJS*, 59, 447
- Jaffe, W., Bremer, M. N., & Baker, K. 2005, *MNRAS*, 360, 748
- Kennicutt, Jr., R. C. 1998, *ARA&A*, 36, 189
- McDonald, M., Bayliss, M., Benson, B. A., Foley, R. J., Ruel, J., Sullivan, P., Veilleux, S., Aird, K. A., Ashby, M. L. N., Bautz, M., Bazin, G., Bleem, L. E., Brodwin, M., Carlstrom, J. E., Chang, C. L., Cho, H. M., Clocchiatti, A., Crawford, T. M., Crites, A. T., de Haan, T., Desai, S., Dobbs, M. A., Dudley, J. P., Egami, E., Forman, W. R., Garmire, G. P., George, E. M., Gladders, M. D., Gonzalez, A. H., Halverson, N. W., Harrington, N. L., High, F. W., Holder, G. P., Holzappel, W. L., Hoover, S., Hrubes, J. D., Jones, C., Joy, M., Keisler, R., Knox, L., Lee, A. T., Leitch, E. M., Liu, J., Lueker, M., Luong-van, D., Mantz, A., Marrone, D. P., McMahon, J. J., Mehl, J., Meyer, S. S., Miller, E. D., Mocanu, L., Mohr, J. J., Montroy, T. E., Murray, S. S., Natoli, T., Padin, S., Plagge, T., Pryke, C., Rawle, T. D., Reichardt, C. L., Rest, A., Rex, M., Ruhl, J. E., Saliwanchik, B. R., Saro, A., Sayre, J. T., Schaffer, K. K., Shaw, L., Shirokoff, E., Simcoe, R., Song, J., Spieler, H. G., Stalder, B., Staniszewski, Z., Stark, A. A., Story, K., Stubbs, C. W., Šuhada, R., van Engelen, A., Vanderlinde, K., Vieira, J. D., Vikhlinin, A., Williamson, R., Zahn, O., & Zenteno, A. 2012a, *Nature*, 488, 349
- McDonald, M., & Veilleux, S. 2009, *ApJ*, 703, L172
- McDonald, M., Veilleux, S., & Mushotzky, R. 2011a, *ApJ*, 731, 33
- McDonald, M., Veilleux, S., Rupke, D. S. N., & Mushotzky, R. 2010, *ApJ*, 721, 1262
- McDonald, M., Veilleux, S., Rupke, D. S. N., Mushotzky, R., & Reynolds, C. 2011b, *ApJ*, 734, 95
- McDonald, M., Wei, L. H., & Veilleux, S. 2012b, *ApJ*, 755, L24
- McNamara, B. R., & Nulsen, P. E. J. 2007, *ARA&A*, 45, 117
- . 2012, *New Journal of Physics*, 14, 055023
- O'Dea, C. P., Baum, S. A., Privon, G., Noel-Storr, J., Quillen, A. C., Zufelt, N., Park, J., Edge, A., Russell, H., Fabian, A. C., Donahue, M., Sarazin, C. L., McNamara, B., Bregman, J. N., & Egami, E. 2008, *ApJ*, 681, 1035
- Oegerle, W. R., Cowie, L., Davidsen, A., Hu, E., Hutchings, J., Murphy, E., Sembach, K., & Woodgate, B. 2001, *ApJ*, 560, 187
- O'Sullivan, E., Giacintucci, S., Babul, A., Raychaudhury, S., Venturi, T., Bildfell, C., Mahdavi, A., Oonk, J. B. R., Murray, N., Hoekstra, H., & Donahue, M. 2012, *MNRAS*, 424, 2971
- Peng, C. Y., Ho, L. C., Impey, C. D., & Rix, H.-W. 2010, *AJ*, 139, 2097
- Peterson, J. R., & Fabian, A. C. 2006, *Phys. Rep.*, 427, 1
- Polletta, M., Tajer, M., Maraschi, L., Trinchieri, G., Lonsdale, C. J., Chiappetti, L., Andreon, S., Pierre, M., Le Fèvre, O., Zamorani, G., Maccagni, D., Garcet, O., Surdej, J., Franceschini, A., Alloin, D., Shupe, D. L., Surace, J. A., Fang, F., Rowan-Robinson, M., Smith, H. E., & Tresse, L. 2007, *ApJ*, 663, 81
- Rawle, T. D., Edge, A. C., Egami, E., Rex, M., Smith, G. P., Altieri, B., Fiedler, A., Haines, C. P., Pereira, M. J., Pérez-González, P. G., Portouw, J., Valtchanov, I., Walth, G., van der Werf, P. P., & Zemcov, M. 2012, *ApJ*, 747, 29
- Rosa-González, D., Terlevich, E., & Terlevich, R. 2002, *MNRAS*, 332, 283
- Salomé, P., & Combes, F. 2003, *A&A*, 412, 657
- Sanders, D. B., & Mirabel, I. F. 1996, *ARA&A*, 34, 749
- Schlegel, D. J., Finkbeiner, D. P., & Davis, M. 1998, *ApJ*, 500, 525
- van Dokkum, P. G. 2001, *PASP*, 113, 1420
- Veilleux, S., Cecil, G., & Bland-Hawthorn, J. 2005, *ARA&A*, 43, 769
- Veilleux, S., Kim, D.-C., Peng, C. Y., Ho, L. C., Tacconi, L. J., Dasrya, K. M., Genzel, R., Lutz, D., & Sanders, D. B. 2006, *ApJ*, 643, 707
- Veilleux, S., Kim, D.-C., & Sanders, D. B. 2002, *ApJS*, 143, 315
- White, D. A., Jones, C., & Forman, W. 1997, *MNRAS*, 292, 419
- Williamson, R., Benson, B. A., High, F. W., Vanderlinde, K., Ade, P. A. R., Aird, K. A., Andersson, K., Armstrong, R., Ashby, M. L. N., Bautz, M., Bazin, G., Bertin, E., Bleem, L. E., Bonamente, M., Brodwin, M., Carlstrom, J. E., Chang, C. L., Chapman, S. C., Clocchiatti, A., Crawford, T. M., Crites, A. T., de Haan, T., Desai, S., Dobbs, M. A., Dudley, J. P., Fazio, G. G., Foley, R. J., Forman, W. R., Garmire, G., George, E. M., Gladders, M. D., Gonzalez, A. H., Halverson, N. W., Holder, G. P., Holzappel, W. L., Hoover, S., Hrubes, J. D., Jones, C., Joy, M., Keisler, R., Knox, L., Lee, A. T., Leitch, E. M., Lueker, M., Luong-Van, D., Marrone, D. P., McMahon, J. J., Mehl, J., Meyer, S. S., Mohr, J. J., Montroy, T. E., Murray, S. S., Padin, S., Plagge, T., Pryke, C., Reichardt, C. L., Rest, A., Ruel, J., Ruhl, J. E., Saliwanchik, B. R., Saro, A., Schaffer, K. K., Shaw, L., Shirokoff, E., Song, J., Spieler, H. G., Stalder, B., Stanford, S. A., Staniszewski, Z., Stark, A. A., Story, K., Stubbs, C. W., Vieira, J. D., Vikhlinin, A., & Zenteno, A. 2011, *ApJ*, 738, 139
- Zauderer, B. A., Veilleux, S., & Yee, H. K. C. 2007, *ApJ*, 659, 1096